

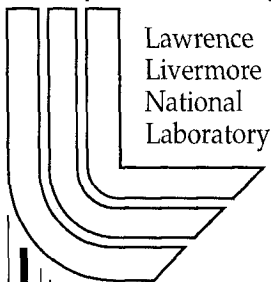
Numerical analysis of spherically convergent Rayleigh-Taylor experiments

*D. Galmiche, C. Cherfils, S.G. Glendinning, B.A. Remington and
A. Richard*

This article was submitted to
*26th European Conference on Laser Interaction with
Matter, Prague, Czech Republic, June 12-16, 2000*

U.S. Department of Energy

May 17, 2000



Lawrence
Livermore
National
Laboratory

DISCLAIMER

This document was prepared as an account of work sponsored by an agency of the United States Government. Neither the United States Government nor the University of California nor any of their employees, makes any warranty, express or implied, or assumes any legal liability or responsibility for the accuracy, completeness, or usefulness of any information, apparatus, product, or process disclosed, or represents that its use would not infringe privately owned rights. Reference herein to any specific commercial product, process, or service by trade name, trademark, manufacturer, or otherwise, does not necessarily constitute or imply its endorsement, recommendation, or favoring by the United States Government or the University of California. The views and opinions of authors expressed herein do not necessarily state or reflect those of the United States Government or the University of California, and shall not be used for advertising or product endorsement purposes.

This is a preprint of a paper intended for publication in a journal or proceedings. Since changes may be made before publication, this preprint is made available with the understanding that it will not be cited or reproduced without the permission of the author.

This report has been reproduced
directly from the best available copy.

Available to DOE and DOE contractors from the
Office of Scientific and Technical Information
P.O. Box 62, Oak Ridge, TN 37831
Prices available from (423) 576-8401
<http://apollo.osti.gov/bridge/>

Available to the public from the
National Technical Information Service
U.S. Department of Commerce
5285 Port Royal Rd.,
Springfield, VA 22161
<http://www.ntis.gov/>

OR

Lawrence Livermore National Laboratory
Technical Information Department's Digital Library
<http://www.llnl.gov/tid/Library.html>

Numerical analysis of spherically convergent Rayleigh-Taylor experiments

D. Galmiche¹, C. Cherfils¹, S.G. Glendinning², B.A. Remington², A. Richard¹

¹ CEA-DAM Ile de France, BP 12, 91680 Bruyères-le-Chatel, France

² LLNL, P.O. Box 808, Livermore, CA 94551, USA

Abstract

In the frame of a CEA/US DOE collaboration, radiation driven spherically convergent experiments were performed on the Nova laser in order to measure the Rayleigh-Taylor growth at the ablation front. Numerical simulations using the 2D Lagrangian code FCI2 have correctly reproduced experiments in moderate convergent geometry [C. Cherfils *et al.*, PRL **83**, 5507 (1999)]. Experiments have addressed convergence ratios up to 4 by considering larger capsules, larger hohlraum and longer laser pulses [S.G. Glendinning *et al.*, to be published in Physics of Plasmas]. Numerical analysis of these high convergence implosions is presented, and the effect of convergence on the Rayleigh-Taylor growth is investigated.

1. Introduction

Spherically convergent experiments were performed on the Nova laser to measure the Rayleigh-Taylor (RT) growth at the ablation front [1-3]. Perturbations, initially located on the surface of doped plastic capsules, were diagnosed by a x-ray backlighting source and imaged by a x-ray camera. By analysing experimental images, we measured, as a function of time, optical depth modulations representative of the perturbation development at the ablation front.

A first set of experiments have addressed moderate convergence ratios at the ablation front close to 2, and weakly nonlinear hydrodynamics. The dominant effect of convergence was simply the shrinking of the wavelength, an effect we denoted as "passive convergence" [2].

The limitation in the observation during the crucial part of the implosion has prompted the change to larger capsule and hohlraum, and longer time scale. More recent experiments allowed us to reach convergence ratios up to 4. We report here the numerical analysis of these last experiments.

2. Spherically convergent experiments

The Nova experimental configuration (Figure 1), typical images and profiles have been detailed in Reference 1. Eight Nova beams are converted to x-rays in a hohlraum, and two other beams, illuminating a separate target (titanium in last experiments), provide a backlighting source to probe the corrugated sphere located in the center of the cavity.

The search for high convergence ratios has led us to consider large capsules coupled to a 4.5 ns shaped laser pulse (Nova "PS35"). The need of a sufficiently large x-ray temperature (160 eV at peak temperature) has imposed to consider a moderately large hohlraum. From the capsule images, most of the Legendre mode 2 distortion is controlled by laser beams pointing, but some distortion at mode 4 was measured (about 8-10% of the radius at latest times).

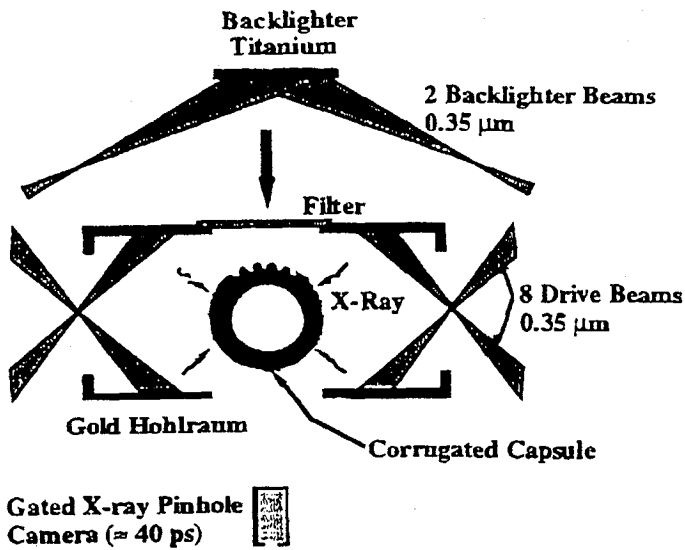


FIG.1. Experimental setup with the capsule at center of hohlraum.

High convergence CH (1.3% Ge) capsules had a 800 μm outer diameter, 42 μm wall thickness, with no fill pressure. They had a square region $120^\circ \times 120^\circ$ with a section of a Legendre mode either 24 or 32, with a peak to valley modulation of 1 μm at the center.

3. Numerical simulations

Simulating the experimental x-ray radiographs was a multistep process. We first estimated a mean radiation drive temperature on the capsule using a tri-dimensional (3D) view factor code. This code included radiative transport but no hydrodynamics. Peak drive temperature is close to 160 eV.

We then used the two-dimensional (2D) radiation hydrodynamics code FCI2 to determine the time-varying spectrum of the drive from a hohlraum simulation assuming cylindrical symmetry. FCI2 is a 2D Lagrangian code including nonlocal thermal equilibrium (non LTE) atomic physics, heat conduction with flux limiting and different radiation transport packages [4, 5]. A multigroup diffusion radiation transport method has been used in our calculations.

The shape and the spectrum of the drive being settled, we used the code FCI2 to simulate the perturbation development during the capsule implosion.

Numerical simulations have evidenced the perturbation growth sensitivity to the spectrum of the incident x-rays. Former shots simulations have been revisited in order to ensure their validity (see Fig. 2). It has appeared that small convergence implosions are not affected by moderate variations in the gold M-band component of the spectrum (says a factor 5 on its level). On the opposite, high convergence implosions are drastically affected by the energy level around the gold M-band range of the spectrum (1.5 keV- 3.6 keV). This behavior is certainly much dependent on the ablator material, and more specifically on its opacity. There exists a *crucial need for confident measurements of instantaneous spectra.*

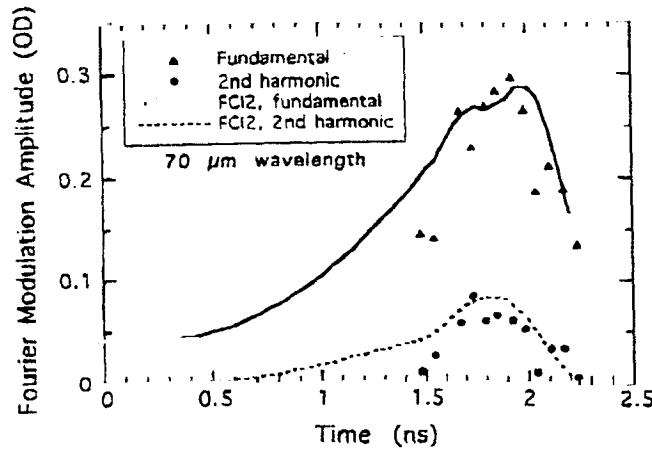


FIG.2. Modulation in optical depth as a function of time for a moderate convergence implosion (530 μm diameter capsule, 70 μm wavelength sinusoidal perturbation, peak to valley amplitude 4 μm).

The plotting symbols represent the experimental results for the fundamental mode (triangles) and the second harmonic (circles). The curves are the corresponding 2D FCI2 simulations.

In this paper, we have considered smoother gold emissivity spectra, in accordance with a work in progress [6], by decreasing the gold M-band energy level obtained in a FCI2 simulation with RADIOM [5].

We have performed simulations of high convergence implosion capsules, being characterized by a Legendre mode 24 perturbation. From the simulation of radiographs, we did a Legendre analysis of the external contour of the capsule, and made a comparison between numerical and experimental data. The agreement on the radius as a position of time is correct (see Fig. 3). We noticed that the time evolution of the radius is weakly dependent on the spectrum of incident x-rays. On the opposite, a suitable spectrum is very important for the simulation of the perturbation growth to compare well with the experimental results (see Fig. 4). An increase of the spectrum in the gold M-band strongly modifies the growth : an increase by a factor 5 in this energy range, leads to a decrease of the growth by a factor 3.

Growth rates are compared with the semi-empirical dispersion relation [7, 8, 9]

$$\gamma = \sqrt{\frac{k}{1 + \frac{g}{kL}} - \beta k v_a}$$

where $\gamma(k, t)$ is the growth rate for wave number k , g is the acceleration, L is the density gradient scale length and v_a is the ablation velocity. When considering a stronger gold M-band, we observe that major effect is a higher ablation velocity, due to the decrease of maximum density. In the same time, as noticed before, time evolution of the ablation front, that is ablation front acceleration, is very weakly influenced. For these reasons, the value of the stabilization term ($\beta k v_a$) increases, and RT growth rate gets much smaller with the stronger preheating. A limit to this analysis is that it has to be pursued in a nonlinear range, out of the scope of this relation.

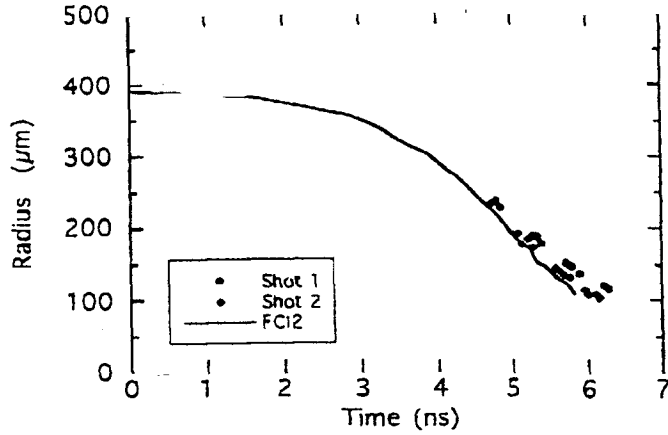


FIG.3. High convergence implosion. Time evolution of the outer radius obtained by analysis of the capsule radiograph in the experiments (symbols) and in the FCI2 simulation (solid curve).

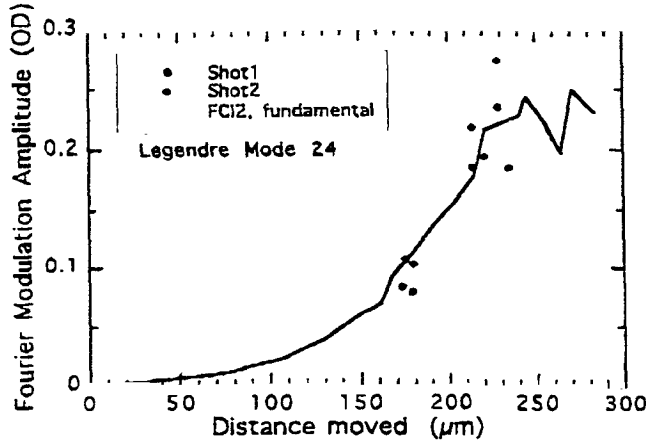


FIG.4. Modulation in optical depth as a function of time for a high convergence implosion (800 μm diameter capsule, mode 24 Legendre perturbation, peak to valley amplitude 1 μm). The plotting symbols represent the experimental results for the fundamental mode. The solid curve is the corresponding 2D FCI2 simulation.

For moderate convergence capsules, the backlighter material is rhodium providing x-rays close to 3 keV, instead of titanium close to 4.7 keV for the high convergence experiments. This is the reason why we observe such a large discrepancy between the initial amplitude in optical depth for the two configurations (see Figures 2 and 4). Growth rate of the modulation amplitude in optical depth is close to 7 with the moderate convergence capsules, but for high convergence capsules it reaches 150.

4. Effect of convergence

Keeping notations introduced in Reference 1, we have compared planar and spherically convergent experiments. P26 and C26 stand respectively for planar and convergent cases obtained with a 2.2 ns shaped laser pulse (Nova "PS26"); C26 corresponds to moderate convergence capsules. C35 stands for high convergence capsules with a laser pulse Nova "PS35".

From the simulations, we consider the evolution of the perturbation amplitudes at the ablation front versus \sqrt{s} , where s is the distance traveled by the ablation front, starting from the time t_0 when the acceleration begins. Using growth factors of spatial amplitude at the ablation surface (ratios of the amplitude to the initial amplitude), determined directly from the

simulations, we observe that the convergent cases grow more rapidly. We reach values of 9 for C26, and 65 for C35 (Fig. 5). When the growth factor is plotted versus $\sqrt{s/\lambda}$, as in Reference 2, the planar and convergent cases appear nearly identical as long as the quantity $\sqrt{s/\lambda}$ stays smaller than 1 (Fig. 5b).

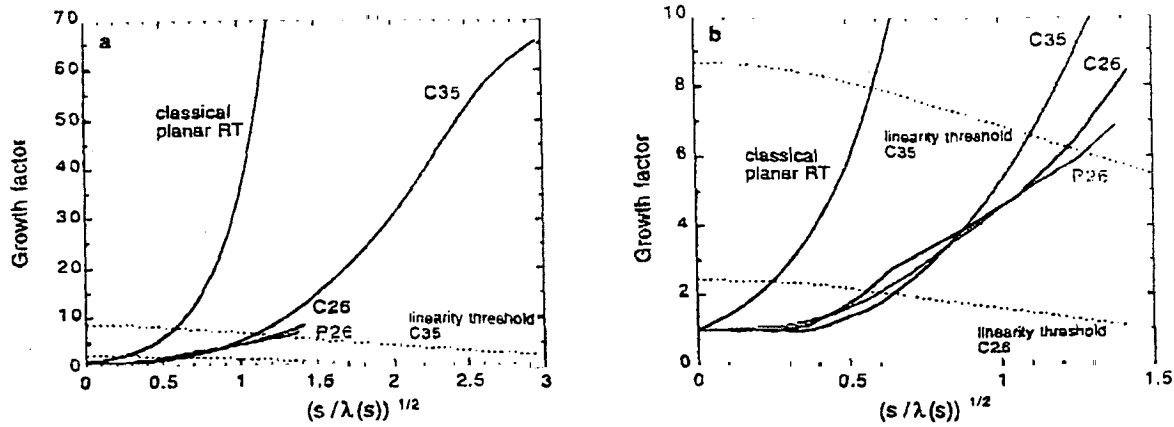


FIG.5. Simulated growth factor versus $\sqrt{s/\lambda}$, where s is the distance accelerated, for the planar (P26) and convergent cases (C26, C35). For small convergence, the dominant effect is the shrinking of the wavelength. Classical RT growth factor and linearity thresholds for the capsules C26 and C35 (when the perturbation amplitude equals 10% of the wavelength) are in dashed lines. Figure 5b is a blow-up of part of figure 5a.

At small convergence, the dominant effect is the shrinking of the wavelength, denoted as “passive convergence” [2]. More recent experiments, as C35 which reaches convergence ratios at the ablation front up to 4, exhibit a major role of the convergence. This is the signature of convergence effects which are important when the radius becomes smaller than half its initial value, denoted as “Bell-Plesset convergence” [10, 11].

This has to be analyzed closely to be clearly evidenced, a major difficulty being the onset of nonlinear saturation. At the beginning, below the linearity threshold, numerical analysis establishes that the growth factor is well matched with the former semi-empirical relation (considering $\beta=1.5-1.7$), without any additive convergence term. For later times, it would be necessary to introduce a convergence term $(R_0/R)^{3/2}$ or $(\rho_0/\rho)(R_0/R)^{3/2}$ to reproduce the fast growth obtained in the simulations, but the linear growth rate relation is no longer valid.

5. Conclusion

Indirect drive experiments have been done on the Nova laser to investigate the role of convergence on RT growth. From numerical simulations, it appears that the perturbation growth at the ablation front can be very sensitive to the spectrum of the incident x-rays, specifically in the case of high convergence experiments. For these experiments, a stronger preheating (factor 5 applied to the gold M-band) does not modify the mean motion of the capsule, but the ablative stabilization term increases, leading to a smaller RT growth rate. The need for confident experimental spectra measurements is emphasized.

Experimental data indicate that convergence effects are important when the radius becomes smaller than half its initial value. For moderate convergence ratios, close to 2, the dominant effect of convergence is simply the shrinking of the wavelength ("passive convergence"). For high convergence ratio, up to 4, spherically convergent geometry effects, as expected from "Bell-Plesset" analysis, are evidenced.

This work was performed under the auspices of the U.S. Department of Energy by the University of California, Lawrence Livermore National Laboratory under Contract No. W-7405-Eng-48.

- [1] S.G. Glendinning *et al.*, to be published in *Physics of Plasmas* (2000).
- [2] C. Cherfils *et al.*, *Phys. Rev. Lett.* **83**, 5507 (1999).
- [3] D. Galmiche *et al.*, in *IFSA99* edited by C. Labaune, W.J. Hogan, K.A. Tanaka (Elsevier, Paris, France, 2000).
- [4] G. Schurtz, in *La Fusion Thermonucléaire Inertielle par Laser*, edited by R. Dautray *et al.* (Eyrolles, Paris, France, 1994), Vol. 2, pp. 1055-1226.
- [5] M. Busquet, *Phys. Fluids B* **5**, 4191 (1993).
- [6] C. Bowen, unpublished work.
- [7] H. Takabe, L. Montierth, R.L. Morse, *Phys. Fluids* **26**, 2299 (1983).
- [8] H. Takabe *et al.*, *Phys. Fluids* **28**, 3676 (1985).
- [9] J. Lindl, *Phys. Plasmas* **2**, 3933 (1995).
- [10] G.I. Bell, Los Alamos National Laboratory, LA-1321 (1951).
- [11] M.S. Plesset, *Journal of Applied Physics* **25**, 96 (1954).